Design of longitudinal autopilot for Sky Sailor UAV using SLC and TECS controllers

Nourddine GHELEM*,[1], Djamal BOUDANA[1], Ouahid BOUCHHIDA[2]

*Corresponding author
*,[1]Department of Engineering, Control Systems and Applied Mathematics, National Polytechnic School ENP of Algiers, Algeria,
nourddine.bg@gmail.com*, boudana_dj@yahoo.fr
[2]Dept. Electrical Engineering LREA Laboratory University of Medea, Medea, Algeria,
bouchhida.ouahid@gmail.com

DOI: 10.13111/2066-8201.2023.15.1.4

Received: 10 February 2023/ Accepted: 24 February 2023/ Published: March 2023

Abstract: *in recent years, UAVs (Unmanned Aerial Vehicle) have become playing an active role and have been involved in a number of fields such as surveillance, photography, agriculture, transportation and communications. For this reason, the research institution is working to develop linear and non-linear controllers to make these UAVs more stable and effective while performing various tasks assigned to them. In this paper, a longitudinal autopilot was designed for a solar UAV (sky sailor) using two controllers, the first is SLC (Successive Loop Closure) which is a classic controller that is based on successive loops with a PID controller, and the second method is the TECS (Total Energy Control System) controller that depends on the total specific energy rate and the energy distribution rate to control the airspeed and altitude of the UAV. After detailing the working principle and tuning of each controller they were applied to the non-linear model of UAV using MATLAB Simulink. Through the results obtained from the simulations, we conclude that the TECS controller is better than the SLC controller in terms of stability and energy economy, being an ideal choice for solar UAVs to increase their endurance, and for civil aircraft to reduce the cost of flights.*

Key Words: *Aircraft Controller, Longitudinal Autopilot, Non-linear Model, TECS Controller, UAV*

1. INTRODUCTION

UAVs have become one of the most popular topics in the field of scientific research due to their inclusion in many fields such as surveillance, photography, agriculture [1], and military applications. This category of aircraft is superior to quadrotors in its ability to carry a significant payload and long flight endurance of up to days for solar aircraft [2].

UAV autopilot designing is a difficult and complex step due to the non-linear behavior of the aircraft and the coupling between variables, inputs and outputs [3]. Over the years, the autopilot for these aircraft was developed using several types of linear controllers, including PID controller [4], LQR controller [5], and non-linear controllers such as backstepping [6], sliding mode [7], and dynamic inversion-based control. The method used to control the aircraft plays a major role in energy consumption, so the control device has a direct impact on the endurance of the aircraft [8]. The Sky Sailor model is a small UAV developed at the University

of Lausanne Technological Institute in 2004;Sky Sailor is a long-endurance solar UAV that uses solar energy to power the propulsion system and electronic devices during the day, while the surplus energy is stored in the battery for night-time use [9]. The main contribution of this work is to design a longitudinal autopilot for the Sky Sailor using two methods: the first is by using an SLC controller, which is a classic method based on a set of closed internal and external loops, and the second method is by using a TESC controller, which depends on balancing between the gravitational force and the lifting force. This controller is often applied to big civil aircraft such as Airbus and Boeing to reduce fuel consumption and cost of flights. In this paper, we applied this controller to a small solar UAV model to increase its endurance; the results obtained using this controller were compared with the results of the classic controller; this paper has been divided into three parts. In the first part, the longitudinal model of Sky Sailor was extracted from the non-linear model [10]; this model was linearized around the equilibrium state, and used to calculate the longitudinal controller by SLC method. To control the altitude of the UAV, there are two inner loops, the first for tuning pitch rate q, the second for tuning the pitch attitude angle θ, and an outer loop for tuning the altitude. As for tuning the airspeed Va of the UAV, there is one loop that uses δt as an input. All of these loops use PID controllers. The second part was devoted to presenting the TECS controller, where a relationship was extracted between the change in the airspeed of UAV and its specified energy rate on the one hand, and the change in the flight path angle $\boldsymbol{\gamma}$ and the distributed energy rate on the other hand. The law control of the airspeed for the UAV was calculated using the specific total energy rate error, and the law control of the altitude was calculated using the distributed energy rate error. After introducing the controllers and calculating the parameters of each one in the first and second parts, in the last part, each method was applied to the non-linear model of Sky Sailor to form a longitudinal autopilot and tuning the airspeed and altitude of it. In the first one, we tested the controllers with a fixed value as input for airspeed and altitude, then we repeated the test by applying a pulse with magnitude + 5 for a short time in the inputs to test the ability of each controller to reject disturbances. Finally, the results obtained by each controller were compared and discussed in terms of performance.

2. LONGITUDINAL AUTOPILOT DESIGN USING SLC (SUCCESSIVE LOOP CLOSURE)

After extracting the non-linear model of Sky-Sailor, which represents ist behavior, in this section we will discuss the development of a longitudinal autopilot using the SLC method, which depends on a set of internal and external closed loops.

To facilitate the study of UAV behavior and the development of a longitudinal autopilot, the dynamic model has been divided into a longitudinal model and a lateral model. Longitudinal dynamics is represented in forward airspeed, climb, descent motion, and angle of inclination [11]. Airspeed plays an important influence on the longitudinal dynamics of an aircraft. Therefore, for longitudinal control, two variables must be controlled, namely the altitude and the air speed. The altitude is adjusted using the attitude angle θ. Airspeed Va can be controlled in two ways: by using the pitch attitude angle θ or by using the throttle. By applying the **SLC** method for the longitudinal control of UAV, it produces four closed loops, the first for tuning the pitch attitude angle θ with respect to the elevator, the second for tuning the altitude with respect to the pitch attitude, the third for tuning the airspeed with respect to the throttle, and the fourth for tuning the airspeed with respect to the pitch attitude [12].
The longitudinal control of the aircraft is carried out in four stages:

- The first is the take-off zone, during which the full value is imposed on the throttle to obtain the highest possible acceleration and imposing a constant value for the pitch attitude.
- The second is the climbing stage, during which the full value of the throttle is maintained while tuning the airspeed using pitch attitude.
- The third stage: When the altitude of the UAV becomes close to the assumed altitude, here the airspeed is tuned using the throttle and the altitude is tuned using pitch attitude.
- The fourth stage is the descent stage, in which the throttle is set to zero, and the airspeed is tuned at the pitch attitude.

In the next step, each closed loop will be dealt separately by extracting the transfer function of each one, then using the PID controllers to form the full longitudinal autopilot.

2.1 Pitch Attitude Hold

To tune the pitch attitude there are two closed loops, the inner one, to set q to δe , and the outer one, to set the θ [13]. We begin by deriving a simplified relationship between the elevator δ_e and the pitch angle θ, and we have:

$$\begin{aligned}\dot{\theta} &= q\cos\,\phi - r\sin\,\phi \\ &= q + q(\cos\,\phi - 1) - r\sin\,\phi \\ &= q + d_{\theta 1}\end{aligned} \tag{1}$$

where $d_{\theta 1} = q(\cos\,\phi - 1) - r\sin\,\phi$ and $d_{\theta 1}$ is small for small roll angles ϕ.
Differentiating, we get

$$\ddot{\theta} = \dot{q} + \dot{d}_{\theta 1}$$

Substituting q, we will get the equation as:

$$\ddot{\theta} = -a_{\theta 1}\dot{\theta} - a_{\theta 2}\theta + a_{\theta 3}\delta_e + d_{\theta 2} \tag{2}$$

where: $a_{\theta 1}, a_{\theta 2}, a_{\theta 3}$ are the pitch dynamics coefficients; they are variables in the aircraft parameters and the trimmed values, $d_{\theta 1}, d_{\theta 2}$ can be considered as a disturbance on the system. Laplace Transfer function is [12]:

$$\theta(s) = \left(\frac{a_{\theta 3}}{s^2 + a_{\theta 1}s + a_{\theta 2}}\right)\left(\delta_e(s) + \frac{1}{a_{\theta 3}}d_{\theta 2}(s)\right) \tag{3}$$

The final numerical transfer function of Pitch (θ) for as input is:

$$\theta(s) = \frac{-66.68}{s^2 + 18.57s + 89.32}\delta_e(s) \tag{4}$$

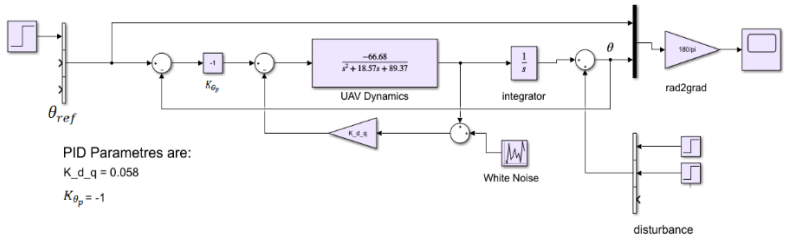

Fig. 1 MATLAB Simulink structure of pitch attitude hold controller

Using the pole placement tuning method in Simulink Matlab, the altitude PID parameters were calculated.

2.2 Altitude Hold Using Commanded Pitch

By applying the SLC strategy to tune the altitude of the UAV using pitch angle θ, it appears that the inner loop is for tuning θ and the outer loop is related to the altitude. In order to adjust the altitude in terms of the pitch angle, a transfer function must be extracted between them, so the following equation of the climbing rate is used, where [12]:

$$\dot{h} = usin\ \theta - vsin\ \phi cos\ \theta - wcos\ \phi cos\ \theta \tag{5}$$

By adding and subtracting $V_a\theta$ we get:

$$\begin{aligned} \dot{h} &= V_a\theta + (usin\ \theta - V_a\theta) - vsin\ \phi cos\ \theta - wcos\ \phi cos\ \theta \\ &= V_a\theta + dh \end{aligned} \tag{6}$$

where:

$$dh = (u\sin\ \theta - V_a\theta) - v\sin\ \phi\cos\ \theta - w\cos\ \phi\cos\ \theta$$

Note that in straight and level flight, where $v \approx 0, w \approx 0, u \approx Va, \varphi \approx 0$ and θ is small, we have $dh \approx 0$.By converting the equation to the Laplace domain, the linearized equation is as follows:

$$h(s) = \frac{V_a}{s}\left(\theta + \frac{1}{V_a}dh\right) \tag{7}$$

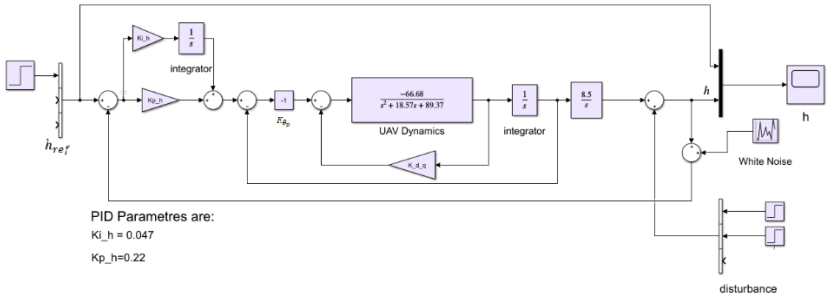

Fig. 2 MATLAB Simulink structure of altitude hold controller

Using the pole placement tuning method in Simulink Matlab, the altitude PID parameters were calculated.

2.3 Airspeed Hold

After extracting an autopilot for adjusting the altitude of the UAV using the pitch angle, autopilot must be extracted to adjust the airspeed in order to complete the longitudinal autopilot.The adjustment of the airspeed is done in two ways: by using the pitch angle, and by using the throttle[14].

2.3.1 Airspeed Hold Using Commanded Pitch

In order to extract the transfer function between the airspeed and the pitch angle, we use aerodynamic expression of velocity in the absence of wind, where [15].

$$V_a = \sqrt{u^2 + v^2 + w^2}$$

This implies that

$$\dot{V}_a = \frac{u\dot{u} + v\dot{v} + w\dot{w}}{V_a} \tag{8}$$

we can express the airspeed vector body-frame components in terms of the airspeed magnitude, angle of attack, and sideslip angle as

$$\begin{pmatrix} u \\ v \\ w \end{pmatrix} = V_a \begin{pmatrix} cos\ \alpha cos\ \beta \\ sin\ \beta \\ sin\ \alpha cos\ \beta \end{pmatrix} \tag{9}$$

Using equation (8), we get [12]:

$$\begin{aligned} \dot{V}_a &= \dot{u}cos\ \alpha cos\ \beta + \dot{v}sin\ \beta + \dot{w}sin\ \alpha cos\ \beta \\ &= \dot{u}cos\ \alpha + \dot{w}sin\ \alpha + dV_1 \end{aligned} \tag{10}$$

where

$$dV_1 = -\dot{u}(1 - \cos\beta)\cos\alpha - \dot{w}(1 - \cos\beta)\sin\alpha + \dot{v}\sin\beta$$

Note that when $\beta = 0$, we have $dV1 = 0$. Substituting equations $\dot{u}$ and $\dot{w}$ in equation (10), we obtain:

$$\dot{V}_a = -av_1 V_a + av_2\delta_t - av_3\theta + d_v \tag{11}$$

av_1, av_2, av_3 They are coefficients in terms of air velocity and dynamic pressure computed at the trimm point. And dV includes $dV2$ as well as the linearization error. In the Laplace domain we have:

$$V_a(s) = \frac{1}{s + av_1}(av_2\delta_t(s) - av_3\theta(s) + d_v(s)) \tag{12}$$

By applying the PID controller, the airspeed can be tuned using the angle θ [12]. In the Laplace domain, we have:

$$V_a(s) = \frac{-K_{\theta_{DC}} g K_{p_{v2}} \left(s + \frac{K_{iv2}}{K_{pv2}}\right)}{s^2 + \left(a_{v1} - K_{\theta_{DC}} g K_{Pv2}\right)s - K_{\theta_{DC}} g K_{iv2}} V_a^c(s) \tag{13}$$

The final numerical transfer function of airspeed (V_a) for as input is:

$$V_a(s) = \frac{2.54s + 4.32}{s^2 + 4.16s + 4.32} V_a^c(s) \tag{14}$$

Depending on the method of imposing roots, the coefficients K_{iv2} and K_{pv2} were calculated so that the bandwidth of the airspeed-from-pitch loop is less than the bandwidth of the pitch stabilization loop, where:

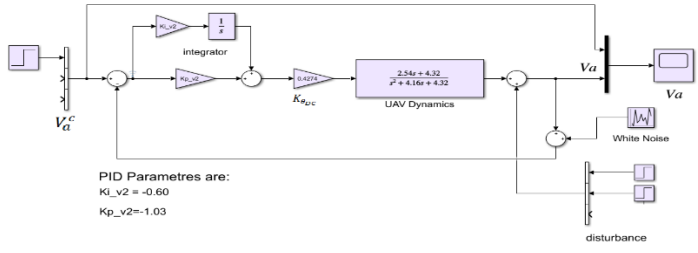

Fig. 3 MATLAB Simulink structure of airspeed hold controller using the pitch angle.

2.3.2 Airspeed Hold Using Throttle

The second way to tune the airspeed of UAV is by using the throttle [12]. Using the PID controller, the airspeed is tuned until it catches up with the control speed.
The following Laplace field transformation equation can be extracted [15]:

$$V_a(s) = \frac{av_2\left(K_{pv}S + K_{iv}\right)}{S^2 + \left(av_1 + av_2K_{pv}\right)S + av_2K_{iv}} V_a^c(s) \tag{15}$$

The final numerical transfer function of airspeed (V_a) for as input is:

$$V_a(s) = \frac{0.18s + 9.98}{s^2 + 1.8s + 9.98} V_a^c(s) \tag{16}$$

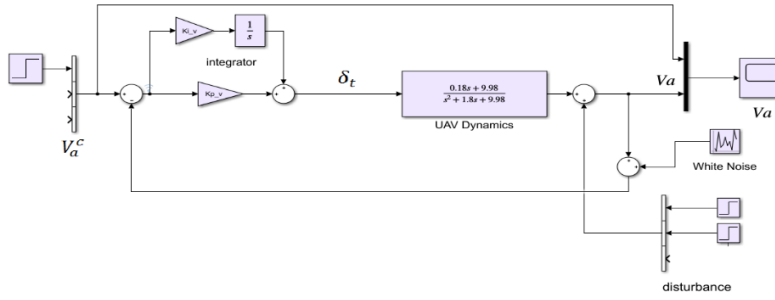

Fig. 4 MATLAB Simulink structure of airspeed hold controller using throttle.

After extracting the controllers for all internal and external loops to tune the altitude of the UAV and its airspeed, they are used in stages to design the full longitudinal autopilot as shown in figure 5 below:

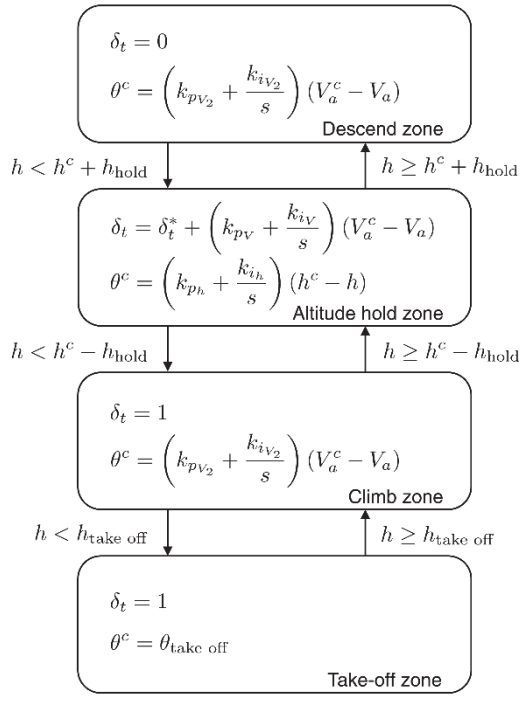

Fig. 5 Structure of the full longitudinal autopilot [12]

3. LONGITUDINAL AUTOPILOT DESIGN USING TECS (TOTAL ENERGY CONTROL SYSTEM)

In this part, a second method for designing the longitudinal autopilot of UAV is discussed, which is the TECS controller. This controller was developed by NASA Langley's Transport System Research Vehicle, by using principles of total energy in which the kinetic and potential energy of the airplane was controlled by the throttle, and the energy distribution is controlled by the elevator [16]. The purpose of developing this controller is to reduce the cost of flights for civil aircraft. It was tested for 3 weeks on the Boeing B737, and it gave good results and proved its performance during experiments. This controller is based on controlling the total power of an aircraft and extracting a law to control airspeed and altitude through the specific energy rate error and the distributed energy rate error. The total energy of an aircraft can be represented by the sum of the kinetic and gravitational energies as follows [16]:

$$E_T = mg\left(\frac{1V^2}{2g} + h\right) \tag{17}$$

Using the small-disturbance theory, the energy of aircraft is linearized at steady flight conditions as:

$$E_{T0} + \Delta E_T = mg\left(\frac{1(V_0 + \Delta V)^2}{2} + (h_0 + \Delta h)\right) \tag{18}$$

where:

V_0 is trimmed airspeed.
E_{T0} is the initial total energy.
ΔE_T is the change in the total energy.
Δh is the change in the flight altitude.

Furthermore, it is assumed that the change in the airspeed $\Delta V^2 = 0$. Deriving Equation (18) with respect to time:

$$\frac{d}{dt}(E_{T0} + \Delta E_T) = mg\frac{d}{dt}\left[\frac{1}{2}\left(\frac{{V_0}^2}{g} + \frac{2V_0\Delta V}{g}\right) + (h_0 + \Delta h)\right] \tag{19}$$

$$\Delta\dot{E} = mg\left(\frac{V_0\Delta\dot{V}}{g} + \Delta\dot{h}\right) \tag{20}$$

Dividing by the trimmed airspeed V_0 yields:

$$\frac{\Delta\dot{E}}{V_0} = mg\left(\frac{\Delta\dot{V}}{g} + \Delta\gamma\right) \tag{21}$$

Where γ is the flight path angle (FPA), which can be expressed in terms of perturbations in pitch attitude θ and incidence α as follows [17]

$$\gamma = \theta - \alpha \tag{22}$$

The α angle can be calculated from the horizontal and vertical velocities. These velocities are obtained from the airspeed sensor. The θ attitude angle can be obtained from the IMU unit. By substituting both angles α and θ in equation (22), the angle γ can be extracted. From equation (21)it can be seen that the rate of change in the total energy of an aircraft is directly related to the rate of change in longitudinal acceleration and the change in flight path angle γ.

By extracting the propeller thrust and replacing it in the equation of longitudinal motion of the UAV, the total energy is calculated as follows:

$$m\Delta\dot{V} = \Delta T - \Delta D - mgsin\ \Delta\gamma \tag{23}$$

Assuming that Δ_γ is small, then $\sin\ \Delta_\gamma = \Delta_\gamma$; therefore:

$$mg\left(\Delta\gamma + \frac{\Delta\dot{V}}{g}\right) = \Delta T - \Delta D \tag{24}$$

Thus, the UAV energy rate is proportional to the difference between thrust T and drag D [18]. Rewriting Equation (24), the thrust changes as:

$$\Delta T = mg\left(\Delta\gamma + \frac{\Delta\dot{V}}{g}\right) + \Delta D = \frac{\Delta\dot{E}_s}{V_0}mg + \Delta D \tag{25}$$

where $\Delta\dot{E}_s$ is the total specific energy rate. Considering that the change in drag force can be neglected in the steady state, it appears that the change in the required force is proportional to the sum of the change of the flight path angle γ and the the specific energy rate [18].

$$\Delta T \propto \left(\Delta\gamma + \frac{\Delta\dot{V}}{g}\right) \tag{26}$$

From equation (25) it can be seen that required thrust is proportional to the specific energy rate, so a control law can be developed that uses throttle to drive the total energy rate error to zero [19], [20].

$$\delta_t = \left(K_{TP} + \frac{K_{TI}}{S}\right)\frac{\dot{E}_{S_E}}{V} \tag{27}$$

where:

K_{TP}, K_{TI} are the throttle proportional and integral gains, respectively.

δ_t is throttle command rate.

$\dot{E}_{S_E}$ is the total specific energy rate error represented by:

$$\frac{\dot{E}_{S_E}}{V} = \left(\frac{\dot{V}_E}{g} + \gamma_E\right) \tag{28}$$

Tuning of the energy rate distribution error can be done by feeding back the difference of the acceleration error term $\frac{\dot{V}_E}{g}$ and the flight path angle error γ_E. Using proportional plus integral control, the elevator control is [20].

$$\delta_e = \left(K_{EP} + \frac{K_{EI}}{S}\right)\left(\frac{\dot{V}_E}{g} - \gamma_E\right) \tag{29}$$

where:

K_{EP}, K_{EI} are elevator proportional and integral gains, respectively.

δ_e is the elevator command rate.

$\dot{V}_E$ is the rate of change of airspeed error.

Relying on equations (27) and (29), the TESC core algorithm can be extracted, as shown in the following figure.

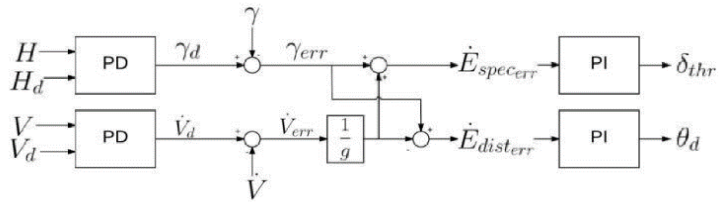

Fig. 6 Total Energy Control System (TECS) core algorithm.

4. RESULTS AND DISCUSSIONS

After introducing each controllers in the first and second parts, extracting the law of controlling airspeed and altitude, calculating parameters of each one, in this part each controller will be tested and their performance evaluated in the presence of external disturbance, as well as the comparison between them and the discussion of the results.

4.1 Altitude Hold and Airspeed Hold Controllers Simulation Tests

In order to evaluate the performance of the two controllers, their ability to tune the altitude and airspeed of the UAV was tested using three methods. The first method addresses the response of the unit step, the second and the third methods test the altitude and the airspeed responses for doublet signal and Multi steps, respectively. These tests were applied to the non-linear model of the UAV.

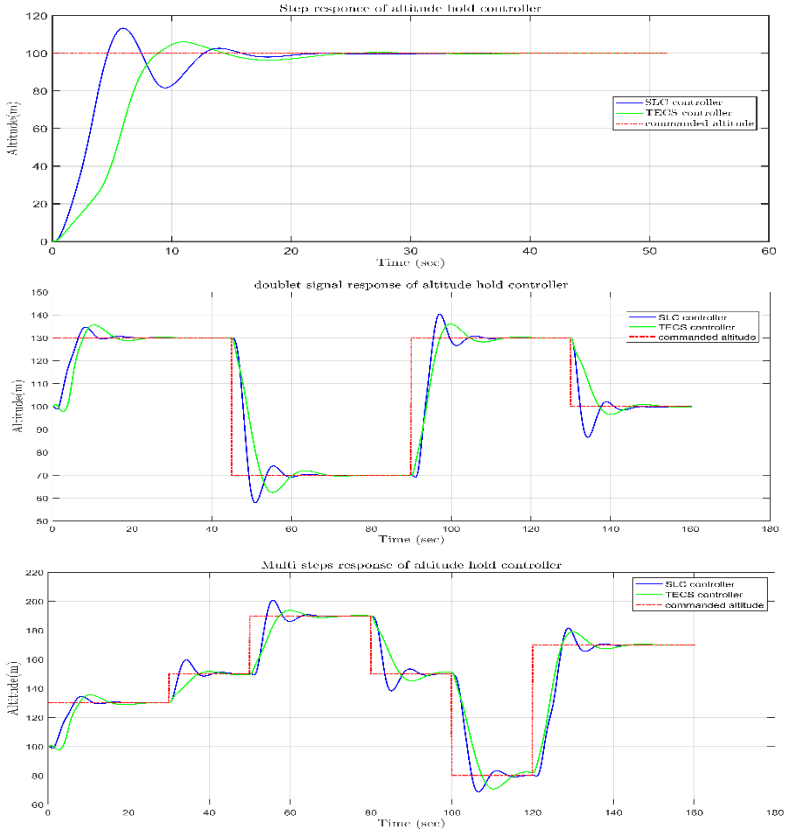

Fig. 7 Altitude Hold Controller Simulation Tests

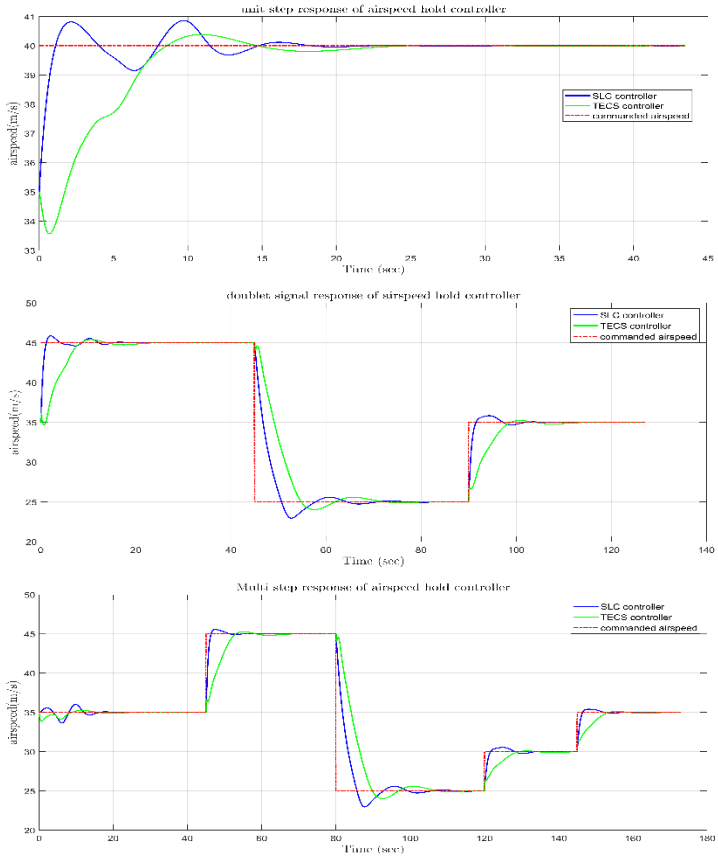

Fig. 8 Airspeed hold controller disturbance rejection

Through the results obtained in figure 7 and figure 8, it appears that the rise time of the SLC controller is better than that of the TECS controller. This is due to the fact that the SCL controller uses the full power of the thrust motor in the climb zone as shown in figure 5. In terms of overshoot, it appears clearly that the TECS controller is better and smoother.

The TECS controller is more stable and energy- efficient than the SLC controller thanks to achieving a balance between gravitational force and lifting force, while the second controller causes a kind of stress to the servomotors and the propulsion motor, so it is therefore more energy consuming.

4.2 The Ability Of The System To Reject The Disturbance

Testing the ability of the controllers to reject the disturbances was done by using the full longitudinal autopilot on the non-linear model of UAV by applying a pulse with magnitude + 5 meters at the altitude state return; and a pulse with magnitude + 5 (m/s) was applied in the return mode of the airspeed.

This test was applied in the unit step response after very steady state. We make a zoom in time from 30 sec to 67 sec as shown in figure 9.

With regard to the ability of each controller to return external disturbances such as sudden weather disturbances or wrong readings of the airspeed and altitude sensors through tests, it is possible to note the superiority of the SLC controller over the TECS controller in terms of speed, but the TECS controller remains better in terms of smoothness and stability.

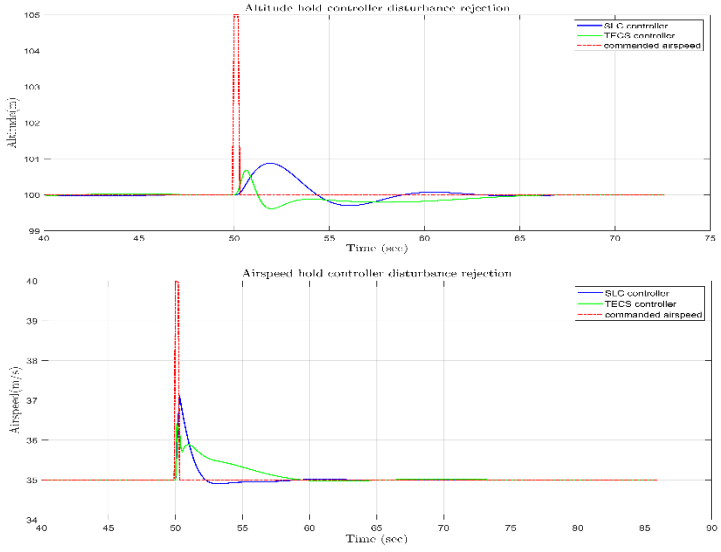

Fig. 9 Altitude hold and airspeed hold controllers disturbance rejection.

5. CONCLUSIONS

Developing effective controllers to ensure the stability of the UAV during missions is one of the most important steps in the process of designing these UAVs. In this paper, two controllers have been developed for longitudinal autopilot of Sky Sailor UAV, the SLC controller and the TECS controller. After calculating the parameters of these controllers, each of them was applied to the non-linear model that represents the UAV, and a set of tests were conducted on each controller to find out their ability to tune airspeed and altitude of the UAV. The ability of each controller to reject external disturbances such as sudden weather turbulence or wrong readings of airspeed and altitude sensors was also tested. Through these tests, it was found that the rise time of the SLC controller is better than that of the TECS controller, but the TECS controller is characterized by smoothness and stability, and it consumes less energy than the first controller.

REFERENCES

[1] J. del Cerro, C. Cruz Ulloa, A. Barrientos, and J. de León Rivas, Unmanned Aerial Vehicles in Agriculture: A Survey, *Agronomy*, vol. **11**, no. 2, p. 203, Jan. 2021.

[2] J. M. Borky, Payload technologies and applications for uninhabited air vehicles (UAVs), *1997 IEEE Aerospace Conference*, Snowmass, CO, USA, 1997, pp. 267-283 vol. **3**, doi: 10.1109/AERO.1997.574874.

[3] M. Liu, G. K. Egan and F. Santoso, Modeling, Autopilot Design, and Field Tuning of a UAV With Minimum Control Surfaces, in *IEEE Transactions on Control Systems Technology*, vol. **23**, no. 6, pp. 2353-2360, Nov. 2015.

[4] E. N. Mobarez, A. Sarhan and M. M. Ashry, Robust PID Flight Controller for Ultrastick-25e UAV, *2019 15th International Computer Engineering Conference (ICENCO)*, Cairo, Egypt, 2019, pp. 150-156.

[5] A. Dharmawan, A. E. Putra, I. M. Tresnayana and W. A. Wicaksono, The Obstacle Avoidance System In A Fixed-Wing UAV When Flying Low Using LQR Method, *2019 International Conference on Computer Engineering, Network, and Intelligent Multimedia (CENIM)*, Surabaya, Indonesia, 2019, pp. 1-7.

[6] M. Lungu, Auto-landing of fixed wing unmanned aerial vehicles using the backstepping control, *ISA Transactions*, vol. **95**, PP. 194-210, 2019.

[7] J. R. Hervas, E. Kayacan, M. Reyhanoglu and H. Tang, Sliding mode control of fixed-wing UAVs in windy environments, *2014 13th International Conference on Control Automation Robotics & Vision (ICARCV)*, Singapore, 2014, pp. 986-991.

[8] E. Bertran and A. Sànchez-Cerdà, On the Tradeoff Between Electrical Power Consumption and Flight Performance in Fixed-Wing UAV Autopilots, in *IEEE Transactions on Vehicular Technology*, vol. **65**, no. 11, pp. 8832-8840, Nov. 2016, doi: 10.1109/TVT.2016.2601927.

[9] A. Noth, W. Engel and R. Siegwart, Flying Solo and Solar to Mars - Global Design of a Solar Autonomous Airplane for Sustainable Flight, *IEEE Robotics & Automation Magazine*, vol. **13**, no. 3, pp. 44-52, Sept. 2006.

[10] A. Noth, S. Bouabdallah, and R. Siegwart, *Dynamic Modeling of Fixed Wing UAVs*, Master Course in Mechanical Department, Autonomous Systems Lab, ETH Zürich, Switzerland, December 2006.

[11] A. E. Ahmed, A. Hafez, A. N. OUDA, *et al,* Modelling of a small unmanned aerial vehicle, *Adv Robot Autom*, vol. **4**, no 126, p. 2, 2015.

[12] R. W. Beard, T. W. Mclain, *Small Unmanned Aircraft: Theory and Practice*, Princeton, NJ: Princeton University Press, 2012.

[13] B. L. Stevens and Frank L. Lewis, *Aircraft control and simulatio*n, John Wiley & Sons, inc, 1992, 617p.

[14] E. A. Ahmed & A. Hafez & A. Ouda & H. Ahmed & H. Abd-Elkader, Design of Longitudinal Motion Controller of a Small Unmanned Aerial Vehicle, *ijisa*, vol. **7**, pp. 37-47, 2015.

[15] D. McLean, *Automatic Flight Control Systems. Coll. Series in Systems and Control Engineering*, Cambridge, U.K., Prentice Hall International, 1990.

[16] A. A. Lambregts, *Total Energy Based Flight Control System*, Patent WO 1984001345, 20 August 1984

[17] M. Cook, *Flight Dynamics Principles*, 3rd ed.; Butter worth Heinemann: Oxford, UK, 2013.

[18] A. A. Lambregts, Vertical Flight Path and Speed Control Autopilot Design Using Total Energy Principles, *Aiaa Guid. Control. Conf. 1983*, vol. **1**, pp. 1–5

[19] L. F. Faleiro, A. A. Lambregts, Analysis and tuning of a Total Energy Control System control law using eigenstructure assignment, *Aerosp. Sci. Technol*, vol. **3**, pp. 5–9, 1999.

[20] K. R. Bruce, NASA B737 Flight Test Results of the Total Energy Control System, In *Proceedings of the Astrodynamics Conference*, Williamsburg, VA, USA, August 1986, pp. 18–20.